

This is an Open Access document downloaded from ORCA, Cardiff University's institutional repository: <https://orca.cardiff.ac.uk/id/eprint/136690/>

This is the author's version of a work that was submitted to / accepted for publication.

Citation for final published version:

Pan, Tao, Sun, Zhonglou, Lai, Xinlei, Orozco Ter Wengel, Pablo , Yan, Peng, Wu, Guiyou, Wang, Hui, Zhu, Weiquan, Wu, Xiaobing and Zhang, Baowei 2019. Hidden species diversity in Pachyhynobius: a multiple approaches species delimitation with mitogenomes. *Molecular Phylogenetics and Evolution* 137 , pp. 138-145. 10.1016/j.ympev.2019.05.005

Publishers page: <http://dx.doi.org/10.1016/j.ympev.2019.05.005>

Please note:

Changes made as a result of publishing processes such as copy-editing, formatting and page numbers may not be reflected in this version. For the definitive version of this publication, please refer to the published source. You are advised to consult the publisher's version if you wish to cite this paper.

This version is being made available in accordance with publisher policies. See <http://orca.cf.ac.uk/policies.html> for usage policies. Copyright and moral rights for publications made available in ORCA are retained by the copyright holders.



1 **Hidden species diversity in *Pachyhynobius*: a multiple**
2 **approaches species delimitation with mitogenomes**

3
4 Tao Pan^{a,b†}, Zhonglou Sun^{a,c†}, Xinlei Lai^a, Pablo Orozco-terWengel^d, Peng Yan^b,
5 Guiyou Wu^a, Hui Wang^a, Weiquan Zhu^c, Xiaobing Wu^{b*}, Baowei Zhang^{a*}

6
7 ^a Anhui Key Laboratory of Eco-engineering and Bio-technique, School of Life
8 Sciences, Anhui University, Hefei 230601, Anhui, China

9 ^b School of Life Sciences, Anhui Normal University, Wuhu 241000, Anhui, China

10 ^c Department of Medicine, University of Utah, Salt Lake City 84112, Utah, United
11 States

12 ^d School of Biosciences, Cardiff University, Cardiff, United Kingdom

13
14 † These authors contributed equally to this work.

15 *Corresponding author

16 E-mail address: zhangbw@ahu.edu.cn (Baowei Zhang), wuxb@ahnu.edu.cn

17 (Xiaobing Wu).

18
19 Running title: Species delimitation of *Pachyhynobius*

20 **ABSTRACT**

21 The lack of distinct morphological features of cryptic species is a hard problem for
22 taxonomy, especially when the taxa are closely related with considerable amounts of
23 ancestral polymorphism. Lately, intensive coalescent-based analyses involving
24 multiple loci have become the preferred method to assess the extent of genetic
25 distinctiveness in otherwise phenotypically similar populations. Previously,
26 phylogenetic studies on *Pachyhynobius shangchengensis* uncovered five extremely
27 deeply divergent clades, which suggested that this species may be a cryptic species
28 complex. In this study, we used the complete mitochondrial genome data and samples
29 from the entire range of stout salamander (*Pachyhynobius*), as well as publicly
30 available mitochondrial genomes to assess species boundaries within this genus using
31 a suite of diverse methodologies (e.g. general mixed Yule coalescent model,
32 Automatic Barcode Gap Discovery). The phylogenetic relationships recovered two
33 major groups within *P. shangchengensis*, with one group formed by four of the six
34 extant populations and corresponding to the central and eastern range of the Dabie
35 mountains, while the other group encompassed two other lineages in the north west of
36 the Dabie mountain range. The species delimitation comparison within
37 *Pachyhynobius* supported the presence of recognized species within the genus, and
38 consensus was observed across methods for the existence of up to five cryptic species
39 within what has been traditionally considered to be *P. shangchengensis*. While this
40 implies the existence of four taxa in addition to the described *P. shangchengensis*
41 species, morphological data and life history information are further required to

42 contribute to the species definition. The observed pattern of genetic variation is likely
43 the outcome of a discontinuous habitat combined with niche conservatism, which
44 produced the sky-island effect observed in *Pachyhynobius*, and which led to
45 formation of a hidden species diversity in this genus.

46

47 **Keywords:** Dabie Mountains; Species delimitation; *Pachyhynobius*; mitochondrial
48 genome; cryptic species.

49

50 **1. Introduction**

51 There is ongoing debate regarding numerous species concepts that emphasize
52 different criteria for delimiting species (Aldhebiani, 2018; Hausdorf, 2011).
53 Regardless of definition, accurate and objective species delimitation is extremely
54 important as species are considered the fundamental unit in many fields such as
55 biogeography, macroevolution, ecology and conservation biology (Agapow et al.,
56 2004; Sites and Marshall, 2003, 2004). Traditionally, species have been identified and
57 described using qualitative or quantitative morphological features (Aldhebiani, 2018;
58 Hausdorf, 2011). For some organisms, the description of independent evolutionary
59 lineages appears to be straightforward due to the existence of diagnostic
60 morphological features that represent different selection trajectories or differences
61 that may have resulted from genetic drift after long-term isolation (Lande, 1976).
62 However, for many organisms, especially those with non-visual mating approaches
63 (Bickford et al., 2007), if the diagnostic morphological features are subtle or even

64 non-existent, species identification based solely on morphological differences may be
65 problematic (Kajtoch et al., 2017; Kotsakiozi et al., 2018; Shirley et al., 2014). In
66 addition, for some organisms, similar selection pressures or extreme environments
67 may result in morphological features experiencing convergent evolution (Nevo, 2001).
68 Morphological variation may be the result of phenotypic plasticity or short-term
69 adaptation to local conditions (Dowle et al., 2015; Svanback and Eklov, 2006;
70 Wagner et al., 2013), a process that further makes species delimitation by
71 morphological differences challenging. Therefore, morphology-based taxonomy may
72 relatively underestimate species number due to the presence of cryptic species, which
73 provide opportunities and challenges for species delimitation based on phylogenetic
74 data (Catarina et al., 2016; Giarla et al., 2014; Kotsakiozi et al., 2018; Sheridan and
75 Stuart, 2018).

76 With the development of species genetic delimitation, various methods have
77 recently been proposed to assess the putative hidden species with evolutionary
78 independence using phylogenetic data. The Bayes factor (BF) approach (Grummer et
79 al., 2013) is based on the marginal-likelihood estimates (MLE) via path-sampling (PS)
80 or stepping-stone sampling (SS) analyses to identify the most suitable species
81 delimitation model across multiple simulated hypotheses (Fan et al., 2011; Li and
82 Drummond, 2012; Xie et al., 2011). Similarly, the Bayesian Phylogenetics and
83 Phylogeography (BPP) is a species-delimitation approach that simultaneously takes
84 into account the phylogenetic uncertainty and stochastic lineage sorting in a dataset to
85 estimate the posterior probability of species assignment, however, conditioning the

86 species assignment to a single user-defined species tree (Yang and Rannala, 2010).
87 BPP estimates the distribution of genealogies for each locus and by testing multiple
88 permutations of the species tree it enables identifying the optimal species delimitation.
89 Coalescent-based methods like the general mixed Yule coalescent model (GMYC)
90 have become an important tree-based species-delimitation approach, although they are
91 often applied to barcoding data, which may not be the most suitable loci for
92 phylogenetic reconstruction (e.g. mitochondrial DNA genes) (Fujisawa and
93 Barraclough, 2013; Fujita and Al, 2012; Leaché and Fujita, 2010; Pons et al., 2006).
94 In GMYC models a maximum likelihood and an ultrametric gene tree is used to
95 simulate the transition threshold between inter- and intra-specific branching patterns,
96 with branching events older than the inferred threshold indicating speciation event,
97 while younger ones represent coalescences within species. For GMYC the putative
98 species number equals the number of lineages crossing the threshold. Similar to
99 GMYC, the Poisson tree processes (PTP/bPTP) model is used to estimate the
100 transition in branch lengths between versus within species (Zhang et al., 2013). PTP
101 calculates the branching process by estimating the expected number of substitutions
102 based on a nonparametric phylogenetic tree. Lastly, Automatic Barcode Gap
103 Discovery (ABGD) employs a different approach, which distinguishes the partitions
104 of the genetic distances among a group of individuals based on clustering algorithms
105 and then infers a final array of putative species (Puillandre et al., 2012a). These
106 species-delimitation methods have been successfully used to identify boundaries for
107 species complexes of morphologically undistinguishable species suggesting that they

108 are fairly robust to model assumptions (Blair and Bryson, 2017; Giarla et al., 2014;
109 Kajtoch et al., 2017; Kotsakiozi et al., 2018; Sheridan and Stuart, 2018; Shirley et al.,
110 2014).

111 The Shangcheng stout salamander (*Pachyhynobius shangchengensis*)
112 (Hynobiidae, Caudata) is a stream salamander, narrowly distributed in high elevation
113 areas in the Dabie Mountains in Eastern China, at the junction of Henan, Hunan and
114 Anhui provinces (Fei et al., 2012). It is endemic to the cool and oxygen-rich mountain
115 streams above 500 meters in elevation. Previously, the subadult of *P.*
116 *shangchengensis* had been recognized as *Hynobius yunanicus* due to the different
117 morphological characters (e.g. white spots on the back and smaller body size)
118 (Nishikawa et al., 2010; Xiong et al., 2007). Currently, *P. shangchengensis* had been
119 classified as Vulnerable (B1ab) by the IUCN
120 (<http://www.iucnredlist.org/details/59109/0>) because of population decline resulting
121 mainly from over-collection for human consumption and habitat loss driven by
122 farming activities and human settlements (Fei et al., 2012). Previous phylogeographic
123 studies of *P. shangchengensis* revealed strong evidence that deep genetic divergences
124 existed among different lineages and that the divergence between clades occurred
125 over one million years ago (Pan et al., 2014; Pan et al., 2019; Zhao et al., 2013).
126 These findings strongly suggest that *Pachyhynobius* may represent a multispecies
127 complex. Consequently, a comprehensive assessment of the species number
128 contextualized with evolutionary history is necessary to disclose the species
129 conservation status, which will contribute to the development of an effective

130 management plan.

131 Here, we sequenced the complete mitochondrial genomes of individuals from six
132 regional populations across the entire range of *P. shangchengensis*, and used them to
133 generate phylogenetic reconstructions of the mitochondrial gene tree. Beyond
134 resolving the phylogenetic relationships in *Pachyhynobius*, the availability of
135 complete mitochondrial genomes can provide sufficient information to reconstruct the
136 evolution and timescale of changes in this genus. In addition, a series of
137 species-delimitation methods were used to clarify species boundaries and to identify
138 candidate species within the genus, *Pachyhynobius*.

139

140 **2. Materials and methods**

141 **2.1. Ethics Statements**

142 In this study, the sample collection was performed by a long-term investigation
143 project on amphibians of Dabie Mountains. This investigation project and the sample
144 collection were approved by Anhui Tianma National Nature Reserve, Anhui Province,
145 China. The relevant document of field permit is provided in the supplementary
146 material.

147

148 **2.2. Sampling**

149 Samples of 35 individuals were collected from 16 locations during 2012-2015 in
150 six isolated geographic areas representing the distribution range of *P.*
151 *shangchengensis*: Jiaoyuan-Tanghui-Xiaolongtan (JTX, 7 individuals),

152 Kangwangzhai- Huangbaishan-Jiufengjian (KHJ, 6 individuals),
153 Mazongling-Wochuan (MW, 6 individuals), Tiantangzhai (TTZ, 8 individuals),
154 Baimajian-Yaoluoping-Mingtangshan (BYM, 7 individuals) and Kujingyuan (KJY, 1
155 individual; Fig. 1). We captured *P. shangchengensis* adults using dip nets and cut the
156 tip of the tail (about 1 cm) prior to releasing them. All samples were preserved in 100%
157 ethanol in the wild and then stored at -80°C until use. Total DNA was extracted from
158 samples using a standard proteinase K/phenol-chloroform protocol (Sambrook et al.,
159 1989). The DNA extraction used EasyPure Purification Kit (TransGene Biotech,
160 Beijing, China) to purify.

161

162 **2.3. PCR amplification**

163 The complete mitochondrial genomes were amplified with PCR using
164 mitochondrial primers designed with Primer Premier version 5.0 based on the
165 mitochondrial genomes of *P. shangchengensis* (NC008080) and *Ranodon sibiricus*
166 (NC004021) (Table S1) (Clarke and Gorley, 2001). PCR reaction mixtures (25 µL)
167 for each gene consisted of 1 µL total DNA (concentration 10-50 ng/µL), 2.5 µL 10×
168 buffer, 1 µL of 2.5 mM MgSO₄, 2 µL of 2 mM dNTPs, 1 U *Taq* polymerase
169 (TransGene Biotech, Beijing, China), 0.3 mM of each primer and sufficient pure
170 molecular biology grade water. The amplification protocol consisted of the following
171 steps: an initial denaturation step of 95°C for 5 min, 32 cycles of denaturation at 95°C
172 for 30 s, primer annealing at 53°C for 30 s and an extension at 72°C for 90 s, and a
173 final extension at 72°C for 10 min. All PCR products were purified with a EasyPure

174 Purification Kit, and sequenced on an ABI Prism 3730 automated sequencer using the
175 BigDye Terminator v3.0 Ready Reaction Cycle Sequencing Kit (Applied
176 Biosystems).

177

178 **2.4. Sequence data preparation**

179 Sequences were assembled with Seqman II (DNASTar, Madison, WI, USA) and
180 visually inspected to ensure the accuracy of variable sites (Burland, 2000). BLAST
181 search and translation test methods were employed to exclude the potential nuclear
182 mitochondrial pseudogenes (Yao et al., 2008). Sequences were aligned using Clustal
183 X version 2.0 (Larkin et al., 2007). The known complete mtDNA sequences of *P.*
184 *shangchengensis* (NC008080) were used to identify protein-coding genes, and the 22
185 tRNA genes were identified by tRNA Scan-SE version 1.21
186 (<http://lowelab.ucsc.edu/tRNAscan-SE> 1.2.1). All assembled and annotated
187 mitochondrial genomes were submitted to GenBank (MK890366-MK890400, Table
188 S2).

189 The complete mitochondrial genomes generated in this study and those of
190 Hynobiidae publicly available in NCBI were used to reconstruct the phylogenetic tree
191 between taxa without partitions using Bayesian methods and Maximum Likelihood
192 (ML), with *Andrias davidianus* and *A. japonicus* as outgroups (Fig. 2). All
193 alignment-ambiguous regions were removed to avoid erroneous phylogenetic
194 hypotheses, and alignment gaps were analyzed as missing data.

195

196 **2.5. Mitochondrial phylogeny**

197 The best-fit DNA sequence evolution model of our dataset was estimated with
198 jModeltest.0.1 using the Bayesian Information Criterion (BIC) to choose the most
199 suitable model (Darriba et al., 2012). The Bayesian phylogenetic tree was inferred
200 using MrBayes version 3.1.2 (<http://mrbayes.csit.fsu.edu/index.php>) (Huelsenbeck
201 and Ronquist, 2001) and the best-fit model identified with jModeltest. Two
202 independent runs of MrBayes' Markov Chain Monte Carlo (MCMC) algorithm were
203 performed to assess convergence of posterior probability distributions. The run
204 parameters used were set 1×10^7 iterations of the MCMC algorithm sampled every
205 1,000 iterations, and discarding the first 10% of the iterations as burn-in. An average
206 standard deviation of split frequencies of 0.01 was used for checking model stability.

207 RaxML version 8 (Stamatakis, 2014) was used to perform ML analyses with a
208 general time reversible model of nucleotide substitution under the Gamma model of
209 rate heterogeneity (i.e., GTRCAT), with 1000 bootstrap iterations to determine
210 internal branch support of the best-scoring tree.

211

212 **2.6. Divergence-Time Analyses**

213 To estimate divergence times between different clades in *Pachyhynobius*, we
214 used BEAST version 1.8.0 (Drummond et al., 2012) to calculate an ultrametric tree
215 using as calibration points information (a, 157.1 Ma, 95% Highest Posterior Density
216 [HPD] = 145.6 – 165.3 Ma; b, 135.1 Ma, 95% HPD = 120.2 – 150.3 Ma; c, 40.2 Ma,
217 95% HPD = 34.5 – 46.2 Ma; Fig. 2) from a previous phylogenetic study of

218 Hynobiidae (Chen et al., 2015). For this analysis, we used a relaxed uncorrelated log
219 normal model of lineage variation, a Yule Process prior for the branching rates, and
220 with a GTR + I + G model of sequence evolution (best selected model). Four
221 replicates of the analysis were run for 1×10^7 generations with parameter and tree
222 sampling every 1,000 generations, discarding the first 25% of BEAST's MCMC
223 iterations as burn-in. Convergence between runs was monitored using Tracer version
224 1.6 (Rambaut et al., 2014) and ESS values indicative of adequate sampling (i.e. >200).
225 The phylogenetic tree was generated and visualized with TreeAnnotator version 1.8.0
226 (Rambaut and Drummond, 2010) and FigTree version 1.4.3 (Rambaut, 2016),
227 respectively. The ultrametric tree without outgroups used for species delimitation was
228 collected from this generated tree.

229

230 **2.7. Species delimitation**

231 We used SPLITSTREE version 4.13.1 (Huson and Bryant, 2006) to construct a
232 phylogenetic network based on uncorrected p-distances with heterozygous
233 ambiguities averaged and normalized, using the neighbor-net ordinary least squares
234 variance and equal angle algorithm and 1,000 bootstrap replicates to assess branch
235 support. We used several species delimitation models to determine the number of
236 different species in our dataset. We used the BF approach (Grummer et al., 2013) to
237 estimate the best fitting model to our dataset between alternative models (M1: 5
238 species; M2: 4 species; M3: 3 species; M4: 1 species) defined by the estimates of
239 population structure identified by the above phylogenetic tree. The MLE of each

240 model was estimated and the BF between pairs of modes was calculated as $BF = 2 \times$
241 $(MLE\ model1 - MLE\ model2)$], with values for BF between 0 and 1 indicating very
242 weak support for model 1 over 2, values between 1 and 3 indicating some support,
243 albeit little, for model 1, values between 3 and 5 indicating strong support for model 1,
244 and values > 5 indicating decisive support for model 1 (Kass and Raftery, 1995). .
245 Two independent runs for each model were performed in *BEAST (Heled and
246 Drummond, 2010) to assess convergence of the MCMC runs. *BEAST was run each
247 time for 1×10^7 generations of the MCMC algorithm sampling every 1,000
248 generations and discarding the first 25% of the iterations as “burn-in”. The general
249 parameter settings were a relaxed uncorrelated log normal model of lineage variation,
250 a Yule Process prior for the branching rates, and with a GTR + I + G model of
251 sequence evolution. For MLE analysis, the applied parameters were as follows: 1×10^6
252 generations, sampling every 1,000 generations and default settings for the other
253 parameters. The results of different runs were combined using LogCombiner. Based
254 on the MLE results, the species tree of *Pachyhynobius* was determined. Convergence
255 of all model parameters was assessed by examining the trace plots and histograms in
256 Tracer.

257 BPP version 3.0 was used to simulate the posterior probabilities of speciation
258 events resulting in fewer or more lineages than the observed data using a reversible
259 jump MCMC (rjMCMC) algorithm (Rannala and Yang, 2003; Yang and Rannala,
260 2010). A guide tree to start the BPP analyses was generated from the species tree
261 estimated with MrBayes. The root age (τ) and prior distributions of the ancestral

262 population size (θ) can affect the posterior probabilities for the BPP models. Due to
263 the lack of knowledge about these parameters in *Pachyhynobius*, we tested the effect
264 of different prior values for τ and θ on the probabilities of posterior speciation. Three
265 ranges for θ were used, i.e. large $G(1, 10)$, middle $\sim G(1, 100)$ and small $\sim G(2, 2000)$
266 ancestral population size, and three ranges for τ representing divergences ranging
267 from deep to shallow genealogies, i.e. $\sim G(1, 10)$, $\tau \sim G(1, 100)$ and $\tau \sim G(2, 2000)$.
268 BPP's run parameters were set to 500,000 generations sampling every 50 steps and
269 discarding the first 100,000 iterations as burn-in. Each BPP analysis of different
270 combinations of θ and τ priors was run twice to test algorithm convergence.

271 In addition to the Bayesian methods tested, we also applied three tree-based
272 species-delimitation methods, namely the single-threshold General Mixed Yule
273 Coalescent (sGMYC) (Pons et al., 2006; Tomochika and Barraclough, 2013), the
274 multiple threshold GMYC (mGMYC) (Monaghan et al., 2009) and Bayesian
275 implementation of the Poisson Tree Processes (bPTP) (Zhang et al., 2013). All three
276 analyses were calculated using the online server (<http://species.h-its.org/>). BEAST's
277 ultrametric tree with an outgroup (*R. sibiricus*) was used for the sGMYC, mGMYC
278 and bPTP models with default parameter settings in the server. The parameters of
279 these three analyses were set as follows: 500,000 generations, a thinning of 500 and
280 burn-in of 10%. Convergence of model was assessed by visualizing plots of MCMC
281 iteration vs. log likelihood. Lastly, we used the computationally efficient
282 distance-based species-delimitation method ABGD (Kekkonen and Hebert, 2014;
283 Puillandre et al., 2012a; Puillandre et al., 2012b), which can quantify the barcode gap

284 location that separates intra- from interspecific distances. During the calculation,
285 default settings were used for the prior range for maximum intraspecific divergence
286 (0.001, 0.1) and minimum slope increase (X) of 1.5 (default) and 1.0. Both JC69 and
287 K80 corrected distances were used to compare species delimitation results.

288

289 **3. Results**

290 **3.1. Sequences variability and trees construction**

291 The aligned mtDNA genome from Hynobiidae and outgroups consisted of 16,575
292 bp nucleotide positions before trimming, and 16,553 bp after trimming. The trimmed
293 data were used for genealogical reconstructions, including 8,105 constant and 8,378
294 variable sites. This dataset yielded well-supported phylogenetic trees (BI and ML; Fig.
295 2) with both reflecting the same topological structure previously identified for
296 Hynobiidae (Chen et al., 2015; Zhang et al., 2006). All *Pachyhynobius* individuals
297 formed a clade that internally presented five well supported groups (posterior
298 probabilities = 1 and bootstrap support values = 100%), each representing a
299 geographical area, namely JTX, KHJ, MW, TTZ and the two sampling areas that
300 could not be genetically told apart, BYM and KJY (Fig. 2). These five lineages
301 grouped forming two branches, one containing the JTX and KHJ lineages, and the
302 other one the remaining 3 groups. The phylogenetic network of *Pachyhynobius*
303 contained the same groupings observed with the phylogenetic methods (Fig. 3).

304 The dating analyses of Hynobiidae suggested that the most recent common
305 ancestor (MRCA) of *Pachyhynobius* dates to ~7.84 million years ago (Ma; 95% HPD

306 = 5.62 – 13.09 Ma; Fig. 2). The MRCA of JTX and KHJ was ~3.19 Ma (95%HPD =
307 1.93 – 5.47 Ma). The MRCA of BYM, MW and TTZ was estimated at ~5.92 Ma (95%
308 HPD = 4.03 – 8.40 Ma), while the MRCA of MW and TTZ was ~3.25 Ma (95% HPD
309 = 2.15 – 5.33 Ma).

310

311 **3.2. Species delimitation**

312 The Bayes Factor for the comparison between the five candidate species
313 hypotheses and either the PS or SS hypotheses was larger than five, indicating that the
314 5-species hypothesis was clearly better than the other two alternatives (Table 1). The
315 BPP analysis supported the BF analysis, with all nine combinations of the values of
316 the priors for τ and θ presenting a posterior probability of at least 0.99 for the
317 hypothesis of 5 species (Table 2). The ABGD analysis suggested a total of five
318 species based on initial partitioning over a range of prior values for the maximum
319 intraspecific divergence observed (Fig. S1). However, as the divergence was reduced,
320 the number of inferred species decreased to three with a maximum intraspecific
321 divergence prior value (P) of 0.0055, or less if a lower threshold was allowed. The
322 sGMYC model yielded 6 clusters and 7 entities. In contrast, the mGMYC model (i.e.
323 several coalescent time values) shows 5 GMYC clusters and 7 entities (Fig. S2). bPTP
324 also suggested a strikingly high number of *Pachyhynobius* species (5) with confidence
325 intervals (4-7) from MCMC analyses (Fig. S3). Overall, the species tree (Fig. 4) was
326 highly consistent with the mtDNA gene tree.

327 Four out of six of the species-delimitation methods consistently identified five

328 species, while the sGMYC and mGMYC identified more than five. The areas of KHJ
329 and MW consistently presented one species per area. However, for both the sGMYC
330 and mGMYC methods the TTZ area presented two candidate species, while the BYM
331 area also presented two species with the sGMYC method, and the JTX area presented
332 two species with the mGMYC method (Table 3). Average pairwise sequence
333 divergence varied markedly among candidate species, from 1.8 % (JTX vs KHJ) to
334 4.1% (KHJ vs MW) (Table 4).

335

336 **4. Discussion**

337 **4.1. Species delimitation of *Pachyhynobius***

338 Generally, one of the main criteria for species delimitation is reciprocal
339 monophyly (Kizirian and Donnelly, 2004). In species delimitation, analytical methods
340 of delimiting species that typically rely upon the genetic distances across lineages or
341 the topological structure of a phylogenetic tree (Sites and Marshall, 2003, 2004)
342 require subjective setting of the thresholds that demarcate the species boundary (Hey,
343 2009). However, for recent speciation events, not all molecular markers are presumed
344 to be reciprocally monophyletic across the phylogenetic tree (Fujita and Al, 2012;
345 Hudson and Coyne, 2002). Recently, it has been possible to identify derived species
346 before achieving reciprocal monophyly after species formation (Knowles and
347 Carstens, 2007). In such cases where there is incomplete lineage sorting,
348 coalescent-based species delimitation approaches can be calculated that do not require
349 reciprocal monophyly of molecular markers or fixed differences (Fujita and Al, 2012;

350 Leaché and Fujita, 2010). In recent years, these methods for species delimitation have
351 been successfully applied to many animal groups, such as sap-green stream frog
352 (Ranidae: *Sylvirana*) (Sheridan and Stuart, 2018), horned lizards (Phrynosomatidae:
353 *Phrynosoma*) (Blair and Bryson, 2017), Kotschy's gecko (Gekkonidae, *Mediodactylus*)
354 (Kotsakiozi et al., 2018), Slender-snouted crocodilian (*Mecistops*
355 *cataphractus*)(Shirley et al., 2014), and Andean mouse opossums (Didelphidae:
356 *Thylamys*)(Giarla et al., 2014). These many examples demonstrate that these methods
357 are successful in delimiting species boundaries for species complexes or
358 morphologically indistinguishable species.

359 In this study we found that the inferred phylogenetic tree for the Chinese
360 salamander *Pachyhynobius* using whole mitochondrial DNA sequences was
361 consistent with previous phylogeographic analyses using single or multiple
362 mitochondrial genes (Pan et al., 2014; Pan et al., 2019; Zhao et al., 2013), confirming
363 the existence of five independent genetic clades within the genus. We found that two
364 areas (KHJ and MW) consistently presented support for the existence of putative
365 species in each of them across the various species-delimitation methods used (Table
366 3). In the species-tree approach (Fig. 4), the statistical support for the three additional
367 lineages of JTX, TTZ, and BYM-KJY was very high (>90%). The signal supporting
368 the identification of a candidate species for each geographic area in the
369 *Pachyhynobius* distribution range was overall strong, as reflected by most
370 species-delimitation methods supporting the presence of five candidate species.
371 However, two of the methods suggested that a further number of hidden species may

372 remain. mGMYC suggested two potential candidate species within the JTX and TTZ
373 lineages, while sGMYC suggested two potential species within the TTZ and BYM
374 lineages. Although it is possible that these two GMYC based methods may be more
375 sensitive to otherwise subtle cryptic divergence in the data, it is also possible that they
376 may be too liberal when defining the number of putative species in a group as has
377 previously been suggested (Blair and Bryson, 2017; Lang et al., 2015). Contrastingly,
378 ABGD based on JC69 and K80 corrected distances indicated that there were fewer
379 species (3 instead of 5), defined as “JTX-KHJ”, “MW-TTZ”, and “BYM-KJY”, or
380 less if lower maximum divergence thresholds were used. These results are
381 conservative in comparison to the GMYC models, and likely representative of the
382 reliance of the ABGD approach just on genetic distances without considering the
383 phylogenetic relationships between the operational taxonomic units studied (Postaire
384 et al., 2016). The genetic distance values among the five lineages were variable,
385 ranging from 1.8% to 4.1%. Overall, the genetic distances were close to intra-genus
386 genetic distances observed in Hynobiidae. For example, in the genus *Hynobius*, the
387 inter-species genetic distances ranged from 1.1% (*H. formosanus* vs *H. arisanensis*) to
388 11.2% (*H. formosanus* vs *H. kimurae*). Therefore, in this study, the species
389 delimitation based on mitochondrial genome data revealed that there are indeed
390 multiple species in *Pachyhynobius*. Of six species-delimitation methods used, four
391 methods strongly supported that there are five determined species (from JTX, KHJ,
392 MW, TTZ, BYM-KJY respectively).

393

394 **4.2. Sky island effect and montane speciation**

395 Abiotic factors such as climate and tectonic events, as well as biological factors
396 such as interspecific or intraspecific interactions, competition and predation, may be
397 the major drivers for biological evolution and diversification temporally and
398 geographically (Benton, 2009). Generally, due to the interactions of multiple abiotic
399 and biological factors, mountains exhibit various microhabitats with different
400 ecological conditions than the surrounding landscape. Herein, unique and endemic
401 species often evolved with the relatively small populations that are separated by
402 well-defined geographical boundaries (Huang et al., 2017; Shepard and Burbrink,
403 2009, 2011). In the vast subtropical regions of China, countless scattered mountains
404 (e.g., Qinling Mountains, Hengduan Mountains, Dabie Mountains) form potential sky
405 islands, which show spatial isolation on restricted areas and are considered ideal
406 natural laboratories for studying the formation of endemic plants and animal species
407 (Gao et al., 2015; Zhen et al., 2016).

408 After the rapid uplift, the Tibetan Plateau and its adjacent mountain ranges acted
409 as a blocky orographic barrier to the atmospheric circulation, and then contributed to
410 the Asian monsoon system (Guo et al., 2008; Song et al., 2010; Tang et al., 2013).
411 During three East Asian monsoon intensification periods (~15 Ma, ~8 Ma and 4-3 Ma)
412 (Jacques et al., 2011; Molnar et al., 2010; Wan et al., 2007), the monsoonal flow led
413 to the humid and warm climate in the south of China (Sun and Wang, 2005). This was
414 favorable for speciation and geographical spreading (Che et al., 2010; Wu et al.,
415 2013). Mountainous areas often harbor more cryptic lineages because altitudinal

416 zonation of habitats and rugged terrain cause the formation of sky island habitats (He
417 and Jiang, 2014; McCormack et al., 2009). For these species restricted to sky-island
418 habitats, dispersal often was limited and more opportunities were created for
419 allopatric divergence, which promotes high levels of inter-population genetic
420 divergence and unique patterns of genetic structure (Favre et al., 2015; Kozak and
421 Wiens, 2006; Pauls et al., 2006; Shepard and Burbrink, 2008, 2009, 2011;
422 Valbuenaureña et al., 2017; Wu et al., 2013; Zhu et al., 2011). For example, in
423 western Arkansas (USA), unique physiographic features of the Ouachita Mountains
424 area, coupled with species response to climatic factors, drove deep lineage divergence
425 in three *Plethodon* species (*P. ouachitae*, *P. fourchensis* and *P. caddoensis*) and
426 finally produced a series of classic phylogeographic structures associated with stream
427 drainages and mountains (Shepard and Burbrink, 2008, 2009, 2011).

428 *Pachyhynobius* is a typical stream salamander, endemic to the Dabie Mountains,
429 and lives in the cool and oxygen-rich streams above 500 meters in elevation (Fei et al.,
430 2012). In this study, dating analyses of Hynobiidae suggested that the MRCA of
431 *Pachyhynobius* dates back to ~7.84 Ma (Fig. 2), while the five candidate species
432 originated ~3.19 to ~5.92 Ma (Fig. 2). The deep genetic divergences were disclosed
433 among these candidate species (Fig. 2, 3 and 4), which indicated that the candidate
434 species may be separated long-term by unsuitable habitats. Dabie Mountains,
435 composed of a chain of ancient isolated low-middle elevation massifs (Fig. 1), were
436 believed to be able to maintain a relatively stable climate over the last several million
437 years (Ju et al., 2007; Zhao et al., 2009). In addition, ecology niche model (ENM)

438 indicated that lower elevation areas acted as a strict and effective isolation barrier for
439 the *Pachyhynobius* species (Pan et al., 2019). Therefore, once discontinuous sky
440 islands were formed and fixed, deep inter-species genetic divergences of
441 *Pachyhynobius* gradually accumulated, then monophyletic groups appeared, and
442 finally, the independent species formed.

443

444 **5. Conclusion**

445 In this study, different species delimitation approaches revealed that multiple
446 species exist in the genus *Pachyhynobius*. Although these methods failed to produce
447 an identical species number, most species delimitation methods indicated that there
448 are five distinct species (from JTX, KHJ, MW, TTZ, BYM-KJY respectively) in
449 *Pachyhynobius*. Discontinuous habitat, combined with niche conservatism, produced
450 the sky-island effect in *Pachyhynobius* and finally led to hidden species diversity in
451 this genus.

452

453 **Author contributions**

454 BWZ led the research team. BWZ, XBW and TP designed the research. TP, ZLS,
455 HW, PY and BWZ collected samples. TP, ZLS and WQZ performed research. TP,
456 XLL, SZL, PY, HW and GYW analyzed data. TP, HW and PO wrote the paper.

457

458 **Funding**

459 This work was supported by the National Natural Science Foundation of China

460 (Grant No. 31272332), National Key Research and Development Program
461 (2016YFC1200705), Anhui Province Higher Education Revitalization Plan, 2014
462 Colleges and Universities Outstanding Youth Talent Support Program, 2017 Anhui
463 Province academic and technical leaders candidates (2017H130), Anhui Natural
464 Science Foundation (Youth, 1908085QC127), Research start-up funds of Anhui
465 Normal University (751865).

466

467 **Acknowledgements**

468 We thank Mr. Zhaojie Peng, Mr. Lifu Qian, Miss Yanan Zhang, Miss Xin Kang
469 for their help in sample collecting and data analysis. We thank Dr. Jackson R.
470 Richards for his linguistic assistance. We thank Associate Editor (Allan Larson) and
471 two anonymous reviewers for their suggestions.

472 **REFERENCES**

- 473 Agapow, P.-M., Bininda-Emonds, O.R.P., Crandall, K.A., Gittleman, J.L., Mace, G.M., Marshall, J.C.,
474 Purvis, A., 2004. The impact of species concept on biodiversity studies. *Q. Rev. Biol.* 79, 161–179.
- 475 Aldhebiani, A.Y., 2018. Species concept and speciation. *Saudi. J. Biol. Sci.* 25, 437–440.
- 476 Benton, M.J., 2009. The Red Queen and the Court Jester: species diversity and the role of biotic and
477 abiotic factors through time. *Science* 323, 728–732.
- 478 Bickford, D., Lohman, D.J., Sodhi, N.S., Ng, P.K.L., Meier, R., Winker, K., Ingram, K.K., Das, I., 2007.
479 Cryptic species as a window on diversity and conservation. *Trends Ecol. Evol.* 22, 148–155.
- 480 Blair, C., Bryson, J.R., 2017. Cryptic diversity and discordance in single-locus species delimitation
481 methods within horned lizards (Phrynosomatidae: *Phrynosoma*). *Mol. Ecol. Res.* 17, 1–15.
- 482 Burland, T.G., 2000. DNASTAR's Lasergene sequence analysis software. *Methods Mol. Biol.* 132, 71–91.
- 483 Catarina, R., David James, H., Salvador, C., Luís, M., Ana, P., 2016. The taxonomy of the *Tarentola*
484 *mauritanica* species complex (Gekkota: Phyllodactylidae): Bayesian species delimitation supports six
485 candidate species. *Mol. Phylogenet. Evol.* 94, 271–278.
- 486 Che, J., Zhou, W.W., Hu, J.S., Yan, F., Papenfuss, T.J., Wake, D.B., Zhang, Y.P., 2010. Spiny frogs (*Paini*)
487 illuminate the history of the Himalayan region and Southeast Asia. *P. Natl. Acad. Sci.* 107, 13765–
488 13770.
- 489 Chen, M.Y., Mao, R.L., Liang, D., Kuro-O, M., Zeng, X.M., Zhang, P., 2015. A reinvestigation of phylogeny
490 and divergence times of Hynobiidae (Amphibia, Caudata) based on 29 nuclear genes. *Mol. Phylogenet.*
491 *Evol.* 83, 1–6.
- 492 Clarke, K.R., Gorley, R.N., 2001. Primer v5. Primer–E Ltd.
- 493 Darriba, D., Taboada, G.L., Doallo, R., Posada, D., 2012. JModelTest 2: more models, new heuristics and
494 parallel computing. *Nat. Methods* 9, 772.
- 495 Dowle, E.J., Morgan-Richards, M., Brescia, F., Trewick, S.A., 2015. Correlation between shell phenotype
496 and local environment suggests a role for natural selection in the evolution of *Placostylus* snails. *Mol.*
497 *Ecol.* 24, 4205–4221.
- 498 Drummond, A.J., Suchard, M.A., Xie, D., Rambaut, A., 2012. Bayesian phylogenetics with BEAUti and
499 the BEAST 1.7. *Mol. Biol. Evol.* 29, 1969–1973.
- 500 Fan, Y., Wu, R., Chen, M.H., Kuo, L., Lewis, P.O., 2011. Choosing among partition models in Bayesian
501 phylogenetics. *Mol. Biol. Evol.* 28, 523–532.
- 502 Favre, A., Päckert, M., Pauls, S.U., Jähnig, S.C., Uhl, D., Michalak, I., Muellner - Riehl, A.N., 2015. The
503 role of the uplift of the Qinghai - Tibetan Plateau for the evolution of Tibetan biotas. *Biol. Rev.* 90,
504 236–253.
- 505 Fei, L., Ye, C.Y., Jiang, J.P., 2012. Colored Atlas of Chinese Amphibians and their Distributions. Sichuan
506 Publishing House of Science and Technology, Chengdu.
- 507 Fujisawa, T., Barraclough, T.G., 2013. Delimiting species using single-locus data and the generalized
508 mixed Yule coalescent approach: a revised method and evaluation on simulated data sets. *Syst. Biol.*
509 62, 707–724.
- 510 Fujita, M.K., Al, E., 2012. Coalescent-based species delimitation in an integrative taxonomy. *Trends*
511 *Ecol. Evol.* 27, 480–488.
- 512 Gao, Y., Ai, B., Kong, H.H., Kang, M., Huang, H.W., 2015. Geographical pattern of isolation and
513 diversification in karst habitat islands: a case study in the *Primulina eburnea* complex. *J. Biogeogr.* 42,
514 2131–2144.

515 Giarla, T.C., Voss, R.S., Jansa, S.A., 2014. Hidden diversity in the Andes: comparison of species
516 delimitation methods in montane marsupials. *Mol. Phylogenet. Evol.* 70, 137–151.

517 Grummer, J.A., Jr, B.R., Reeder, T.W., 2013. Species delimitation using Bayes factors: simulations and
518 application to the *Sceloporus scalaris* species group (Squamata: Phrynosomatidae). *Syst. Biol.* 63, 119–
519 133.

520 Guo, Z.T., Sun, B., Zhang, Z.S., Peng, S.Z., Xiao, G.Q., Ge, J.Y., Hao, Q.Z., Qiao, Y.S., Liang, M.Y., Liu, J.F.,
521 2008. A major reorganization of Asian climate by the early Miocene. *Clim. Past* 4, 153–174.

522 Hausdorf, B., 2011. Progress toward a general species concept. *Evolution* 65, 923–931.

523 He, K., Jiang, X.L., 2014. Sky islands of southwest China. I: an overview of phylogeographic patterns.
524 *Chinese Sci. Bull.* 59, 585 – 597.

525 Heled, J., Drummond, A.J., 2010. Bayesian inference of species trees from multilocus data. *Mol. Biol.*
526 *Evol.* 27, 570–580.

527 Hey, J., 2009. *On the arbitrary identification of real species.* Cambridge University Press, Cambridge,
528 UK.

529 Huang, Z.S., Yu, F.L., Gong, H.S., Song, Y.L., Zeng, Z.G., Zhang, Q., 2017. Phylogeographical structure
530 and demographic expansion in the endemic alpine stream salamander (Hynobiidae: *Batrachuperus*) of
531 the Qinling Mountains. *Sci. Rep.* 7, 1–13.

532 Hudson, R.R., Coyne, J.A., 2002. Mathematical consequences of the genealogical species concept.
533 *Evolution* 56, 1557–1565.

534 Huelsenbeck, J.P., Ronquist, F., 2001. MrBayes: Bayesian inference of phylogenetic trees.
535 *Bioinformatics* 17, 754–755.

536 Huson, D.H., Bryant, D., 2006. Application of phylogenetic networks in evolutionary studies. *Mol. Biol.*
537 *Evol.* 23, 254–267.

538 Jacques, F.M.B., Guo, S.X., Su, T., Xing, Y.W., Huang, Y.J., Liu, Y.S., Ferguson, D.K., Zhou, Z.K., 2011.
539 Quantitative reconstruction of the Late Miocene monsoon climates of southwest China: a case study
540 of the Lincang flora from Yunnan Province. *Palaeogeogr. Palaeoclimatol.* 304, 318–327.

541 Ju, L., Wang, H., Jiang, D., 2007. Simulation of the Last Glacial Maximum climate over East Asia with a
542 regional climate model nested in a general circulation model. *Palaeogeogr. Palaeoclimatol.* 248, 376–390.

543 Kajtoch, Ł., Montagna, M., Wanat, M., 2017. Species delimitation within the *Bothryorrhynchapion*
544 weevils: Multiple evidence from genetics, morphology and ecological associations. *Mol. Phylogenet.*
545 *Evol.* 120, 354–363.

546 Kass, R.E., Raftery, A.E., 1995. Bayes factors. *J. Am. Stat. Assoc.* 90, 773–795.

547 Kekkonen, M., Hebert, P.D., 2014. DNA barcode-based delineation of putative species: efficient start
548 for taxonomic workflows. *Mol. Ecol. Res.* 14, 706–715.

549 Kizirian, D., Donnelly, M.A., 2004. The criterion of reciprocal monophyly and classification of nested
550 diversity at the species level. *Mol. Phylogenet. Evol.* 32, 1072–1076.

551 Knowles, L.L., Carstens, B.C., 2007. Delimiting species without monophyletic gene trees. *Syst. Biol.* 56,
552 887–895.

553 Kotsakiozi, P., Jablonski, D., Ilgaz, Ç., Kumlutaş, Y., Avci, A., Meiri, S., Itescu, Y., Kukushkin, O., Gvoždík,
554 V., Scillitani, G., 2018. Multilocus phylogeny and coalescent species delimitation in Kotschy's gecko,
555 *Mediodactylus kotschy*: hidden diversity and cryptic species. *Mol. Phylogenet. Evol.* 125, 177–187.

556 Kozak, K.H., Wiens, J.J., 2006. Does niche conservatism promote speciation? A case study in North
557 American salamanders. *Evolution* 60, 2604–2621.

558 Lande, R., 1976. Natural selection and random genetic drift in phenotypic evolution. *Evolution* 30,

559 314–334.

560 Lang, A.S., Bocksberger, G., Stech, M., 2015. Phylogeny and species delimitations in European
561 *Dicranum* (Dicranaceae, Bryophyta) inferred from nuclear and plastid DNA Mol. Phylogenet. Evol. 92,
562 217–225.

563 Larkin, M.A., Blackshields, G., Brown, N.P., Chenna, R., McGettigan, P.A., McWilliam, H., Valentin, F.,
564 Wallace, I.M., Wilm, A., Lopez, R., Thompson, J.D., Gibson, T.J., Higgins, D.G., 2007. Clustal W and
565 Clustal X version 2.0. *Bioinformatics* 23, 2947–2948.

566 Leaché, A.D., Fujita, M.K., 2010. Bayesian species delimitation in West African forest geckos
567 (*Hemidactylus fasciatus*). *P. Roy. Soc. Lond. B Biol.* 277, 3071–3077.

568 Li, W.L.S., Drummond, A.J., 2012. Model averaging and Bayes factor calculation of relaxed molecular
569 clocks in Bayesian phylogenetics. *Mol. Biol. Evol.* 29, 751–761.

570 McCormack, J.E., Huang, H., Knowles, L.L., Gillespie, R., Clague, D., 2009. Sky islands. *Encyclopedia of*
571 *Islands* 4, 841–843.

572 Molnar, P., Boos, W.R., Battisti, D.S., 2010. Orographic controls on climate and paleoclimate of Asia:
573 thermal and mechanical roles for the Tibetan Plateau. *Annu. Rev. Earth Pl. Sc.* 38, 77–102.

574 Monaghan, M.T., Wild, R., Elliot, M., Fujisawa, T., Balke, M., Inward, D.J.G., Lees, D.C., Ranaivosolo, R.,
575 Eggleton, P., Barraclough, T.G., 2009. Accelerated species inventory on Madagascar using
576 coalescent-based models of species delineation. *Syst. Biol.* 58, 298–311.

577 Nevo, E., 2001. Evolution of genome-phenome diversity under environmental stress. *Proc. Natl. Acad.*
578 *Sci.* 98, 6233–6240.

579 Nishikawa, K., Jiang, J.P., Matsui, M., Mo, Y.M., Chen, X.H., Kim, J.B., Tominaga, A., Yoshikawa, N., 2010.
580 Invalidation of *Hynobius yunanicus* and molecular phylogeny of *Hynobius* salamander from continental
581 China (Urodela, Hynobiidae). *Zootaxa* 2426, 65–67.

582 Pan, T., Wang, H., Hu, C.C., Shi, W.B., Zhao, K., Huang, X., Zhang, B.W., 2014. Range-wide
583 phylogeography and conservation genetics of a narrowly endemic stream salamander, *Pachyhynobius*
584 *shangchengensis* (Caudata, Hynobiidae): implications for conservation. *Genet. Mol. Res.* 13, 2873–
585 2885.

586 Pan, T., Wang, H., Pablo, O., Hu, C.C., Wu, G.Y., Qian, L.F., Sun, Z.L., Shi, W.B., Yan, P., Wu, X.B., Zhang,
587 B.W., 2019. Long-term sky islands generate highly divergent lineages of a narrowly distributed stream
588 salamander (*Pachyhynobius shangchengensis*) in mid-latitude mountains of East Asia. *BMC Evol. Biol.*
589 (Accepted).

590 Pauls, S.U., Lumbsch, T., Haase, P., 2006. Phylogeography of the montane caddisfly *Drusus discolor*:
591 evidence for multiple refugia and periglacial survival. *Mol. Ecol.* 15, 2153–2169.

592 Pons, J., Barraclough, T.G., Gomez-Zurita, J., Cardoso, A., Duran, D.P., Hazell, S., Kamoun, S., Sumlin,
593 W.D., Vogler, A.P., 2006. Sequence-based species delimitation for the DNA taxonomy of undescribed
594 insects. *Syst. Biol.* 55, 595–609.

595 Postaire, B., Magalon, H., Bourmaud, A.F., Bruggemann, J.H., 2016. Molecular species delimitation
596 methods and population genetics data reveal extensive lineage diversity and cryptic species in
597 Aglaopheniidae (Hydrozoa). *Mol. Phylogenet. Evol.* 105, 36–49.

598 Puillandre, N., Lambert, A., Brouillet, S., Achaz, G., 2012a. ABGD, Automatic Barcode Gap Discovery for
599 primary species delimitation. *Mol. Ecol.* 21, 1864–1877.

600 Puillandre, N., Modica, M.V., Zhang, Y., Sirovich, L., Boisselier, M.C., Cruaud, C., Holford, M., Samadi, S.,
601 2012b. Large-scale species delimitation method for hyperdiverse groups. *Mol. Ecol.* 21, 2671–2691.

602 Rambaut, A., 2016. FigTree v1.4.3; 2016. Available at: <http://tree.bio.ed.ac.uk/software/figtree/>.

603 Rambaut, A., Drummond, A.J., 2010. TreeAnnotator version 1.8; 2016. Available at:
604 <http://beast.community/programs>.

605 Rambaut, A., Suchard, M., Xie, D., Drummond, A.J., 2014. MCMC Trace Analysis Package (version 1.6);
606 2014. Available at: <http://tree.bio.ed.ac.uk/software/tracer/>.

607 Rannala, B., Yang, Z.H., 2003. Bayes estimation of species divergence times and ancestral population
608 sizes using DNA sequences from multiple loci. *Genetics* 164, 1645-1656.

609 Sambrook, J., Fritsch, E.F., Maniatis, T., 1989. *Molecular cloning*. Cold Spring Harbor Laboratory Press,
610 New York.

611 Shepard, D.B., Burbrink, F.T., 2008. Lineage diversification and historical demography of a sky island
612 salamander, *Plethodon ouachitae*, from the Interior Highlands. *Mol. Ecol.* 17, 5315 – 5335.

613 Shepard, D.B., Burbrink, F.T., 2009. Phylogeographic and demographic effects of Pleistocene climatic
614 fluctuations in a montane salamander, *Plethodon fourchensis*. *Mol. Ecol.* 18, 2243–2262.

615 Shepard, D.B., Burbrink, F.T., 2011. Local-scale environmental variation generates highly divergent
616 lineages associated with stream drainages in a terrestrial salamander, *Plethodon caddoensis*. *Mol.*
617 *Phylogenet. Evol.* 59, 399–411.

618 Sheridan, J.A., Stuart, B.L., 2018. Hidden species diversity in *Sylvirana nigrovittata* (Amphibia: Ranidae)
619 highlights the importance of taxonomic revisions in biodiversity conservation. *PLoS One* 13, e0192766.

620 Shirley, M.H., Vliet, K.A., Carr, A.N., Austin, J.D., 2014. Rigorous approaches to species delimitation
621 have significant implications for African crocodylian systematics and conservation. *Proc. Biol. Sci.* 281,
622 20132483.

623 Sites, J.W., Marshall, J.C., 2003. Delimiting species: a renaissance issue in systematic biology. *Trends*
624 *Ecol. Evol.* 18, 462–470.

625 Sites, J.W., Marshall, J.C., 2004. Operational criteria for delimiting species. *Ann. Rev. Ecol. Evol. Syst.* 35,
626 199–227.

627 Song, J.H., Kang, H.S., Byun, Y.H., Hong, S.Y., 2010. Effects of the Tibetan Plateau on the Asian summer
628 monsoon: a numerical case study using a regional climate model. *Int. J. Climatol.* 30, 743–759.

629 Stamatakis, A., 2014. RaxML version 8: a tool for phylogenetic analysis and post-analysis of large
630 phylogenies. *Bioinformatics* 30, 1312–1313.

631 Sun, X.G., Wang, P.X., 2005. How old is the Asian monsoon system?—Palaeobotanical records from
632 China. *Palaeogeogra. Palaeocl.* 222, 181–222.

633 Svanback, R., Eklov, P., 2006. Genetic variation and phenotypic plasticity: causes of morphological and
634 dietary variation in Eurasian perch. *Evol. Ecol. Res.* 8, 37–49.

635 Tang, H., Micheels, A., Eronen, J.T., Ahrens, B., Fortelius, M., 2013. Asynchronous responses of East
636 Asian and Indian summer monsoons to mountain uplift shown by regional climate modelling
637 experiments. *Clim. Dynam.* 40, 1531–1549.

638 Tomochika, F., Barraclough, T.G., 2013. Delimiting species using single-locus data and the generalized
639 mixed Yule coalescent approach: a revised method and evaluation on simulated data sets. *Syst. Biol.*
640 62, 707–724.

641 Valbuenaureña, E., Solermembrives, A., Steinfartz, S., Orozcoterwengel, P., Carranza, S., 2017. No signs
642 of inbreeding despite long-term isolation and habitat fragmentation in the critically endangered
643 Montseny brook newt (*Calotriton arnoldi*). *Heredity* 118, 1–12.

644 Wagner, C.E., Keller, I., Wittwer, S., Selz, O.M., Mwaiko, S., Greuter, L., Sivasundar, A., Seehausen, O.,
645 2013. Genome-wide RAD sequence data provide unprecedented resolution of species boundaries and
646 relationships in the Lake Victoria cichlid adaptive radiation. *Mol. Ecol.* 22, 787–798.

647 Wan, S.M., Li, A.C., Clift, P.D., Stuut, J.B.W., 2007. Development of the East Asian monsoon:
648 mineralogical and sedimentologic records in the northern South China Sea since 20 Ma. *Palaeogeogra.*
649 *Palaeocl.* 254, 561–582.

650 Wu, Y.K., Wang, Y.Z., Jiang, K., Hanken, J., 2013. Significance of pre-Quaternary climate change for
651 montane species diversity: insights from Asian salamanders (Salamandridae: *Pachytriton*). *Mol.*
652 *Phylogenet. Evol.* 66, 380–390.

653 Xie, W.G., Lewis, P.O., Fan, Y., Kuo, L., Chen, M.H., 2011. Improving marginal likelihood estimation for
654 Bayesian phylogenetic model selection. *Syst. Biol.* 60, 150–160.

655 Xiong, J.L., Chen, Q., Zeng, X.M., Zhao, E.M., Qing, L.Y., 2007. Karyotypic, Morphological, and
656 Molecular Evidence for *Hynobius yunanicus* as a Synonym of *Pachyhynobius shangchengensis* (Urodela:
657 Hynobiidae). *J. Herpetol.* 41, 664–671.

658 Yang, Z.H., Rannala, B., 2010. Bayesian species delimitation using multilocus sequence data. *P. Natl.*
659 *Acad. Sci. USA* 107, 9264–9269.

660 Yao, Y.G., Kong, Q.P., Salas, A., Bandelt, H.J., 2008. Pseudomitochondrial genome haunts disease
661 studies. *J. Med. Genet.* 45, 769–772.

662 Zhang, J., Kapli, P., Pavlidis, P., Stamatakis, A., 2013. A general species delimitation method with
663 applications to phylogenetic placements. *Bioinformatics* 29, 2869–2876.

664 Zhang, P., Chen, Y.Q., Zhou, H., Liu, Y.F., Wang, X.L., Papenfuss, T.J., Wake, D.B., Qu, L.H., 2006.
665 Phylogeny, evolution, and biogeography of Asiatic salamanders (Hynobiidae). *P. Natl. Acad. Sci. USA*
666 103, 7360–7365.

667 Zhao, B., Zhang, J., Sun, X.H., 2009. Eco-environmental vulnerability evaluation based on GIS in
668 Tongbai–Dabie Mountain area of Huai River Basin. *Res. Soil Water Conserv.* 16, 135–138.

669 Zhao, Y.Y., Zhang, Y.H., Li, X.C., 2013. Molecular phylogeography and population genetic structure of an
670 endangered species *Pachyhynobius shangchengensis* (hynobiid Salamander) in a fragmented habitat
671 of southeastern China. *PLoS One* 8, e78064.

672 Zhen, Y., Chen, P.P., Bu, W.J., 2016. Terrestrial mountain islands and Pleistocene climate fluctuations as
673 motors for speciation: a case study on the genus *Pseudovelia* (Hemiptera: Veliidae). *Sci. Rep.* 6, 33625.

674 Zhu, L.F., Zhang, S.N., Gu, X.D., Wei, F.W., 2011. Significant genetic boundaries and spatial dynamics of
675 giant pandas occupying fragmented habitat across southwest China. *Mol. Ecol.* 20, 1122–1132.

676

677

678 **Titles and legends to figures**

679 **Fig. 1:** Sampling area and regional group of *Pachyhynobius* in Dabie Mountains,
680 China. The dotted lines represent rivers. The values with different colors
681 represent the elevations of mountains. Sampling sites are shown as ellipses. The
682 approximate position of the region within China is shown in the inset as a green
683 square.

684

685 **Fig. 2:** Mitochondrial genomic phylogeny of the Hynobiidae. The species from
686 *Pachyhynobius* are shown with a pink background. The values on nodes indicate
687 Bayesian posterior probabilities and ML bootstrap support (shown as a
688 percentage). These letters (a, b and c) indicate the calibration points. The blue
689 lines on nodes correspond to the 95% highest posterior density of the age of the
690 node. The bottom axis is in millions of years.

691

692 **Fig. 3:** Network constructed from the complete mitochondrial genome of the
693 *Pachyhynobius* samples based on uncorrected p-distances using SPLITSTREE.
694 The values on nodes indicate bootstrap support (only values above 75% are
695 shown).

696

697 **Fig. 4:** Species tree estimated using BEAST based on complete mitochondrial
698 genome in *Pachyhynobius*. The values on nodes are Bayesian posterior
699 probabilities.

700

701 **Fig. S1:** Species delimitation analyses by ABGD methods with two model (JC90 and
702 K801) based on complete mitochondrial genome in *Pachyhynobius*. Y-axis shows
703 the number of groups inferred, and the x-axis the maximum divergence threshold
704 used for species delimitation. The two models show identical results of species
705 delimitation.

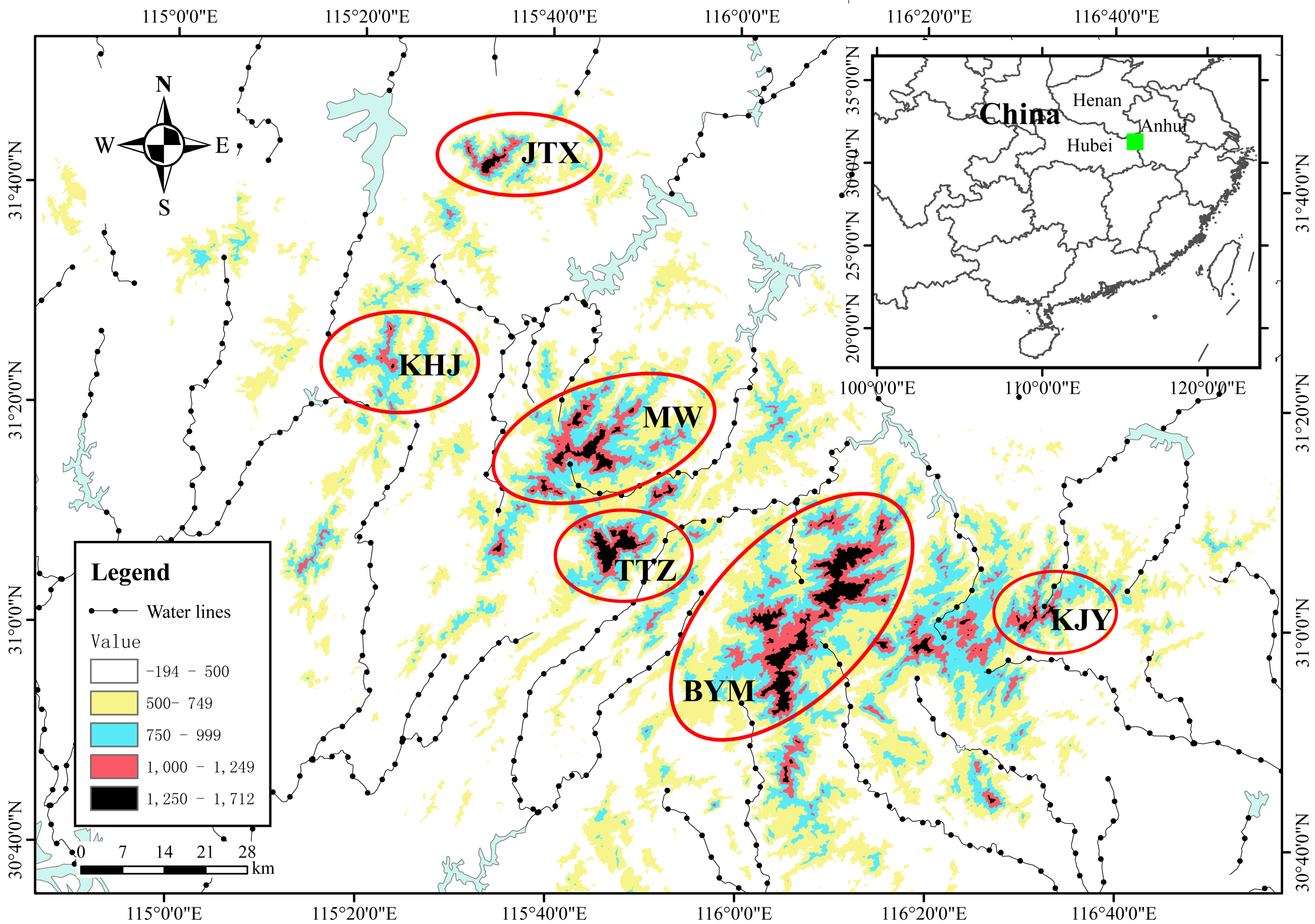
706

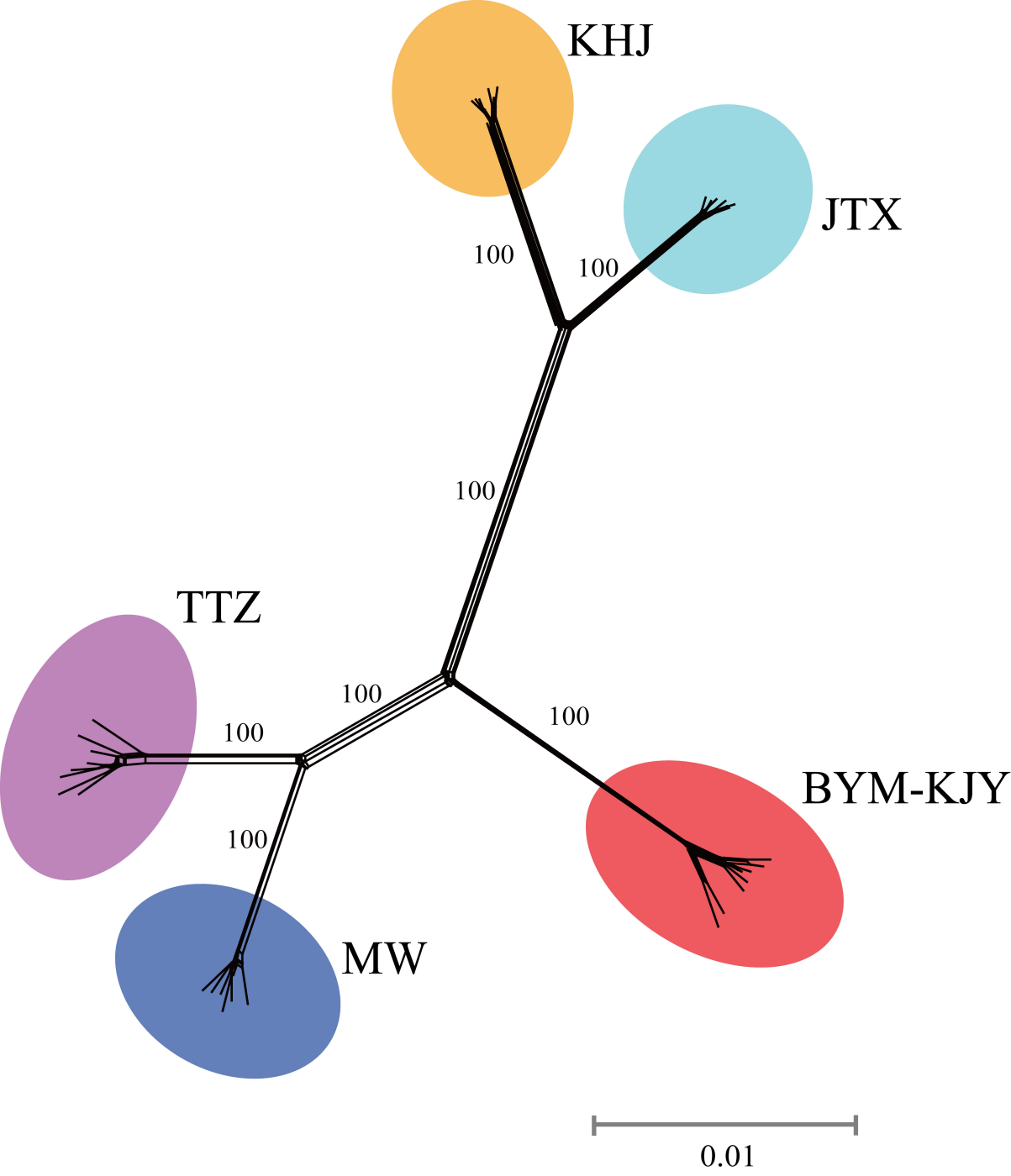
707 **Fig. S2:** Lineage through time plots in the species delimitation analyses by sGMYC
708 method (A) and mGMYC method (B) based on complete mitochondrial genomes
709 in *Pachyhynobius*. N represents the lineage number. Vertical red line(s) indicate
710 the inflection point between speciation and coalescence. Branching events older
711 than the inferred threshold indicating speciation event, while younger ones
712 representing coalescences within species. The bottom axis is in millions of years.

713

714 **Fig. S3:** Species delimitation analyses by bPTP methods based on complete
715 mitochondrial genomes in *Pachyhynobius*. The putative molecular species
716 identified are marked beside the tree. The numbers above branches correspond to
717 the nodes' support posterior probabilities.

718





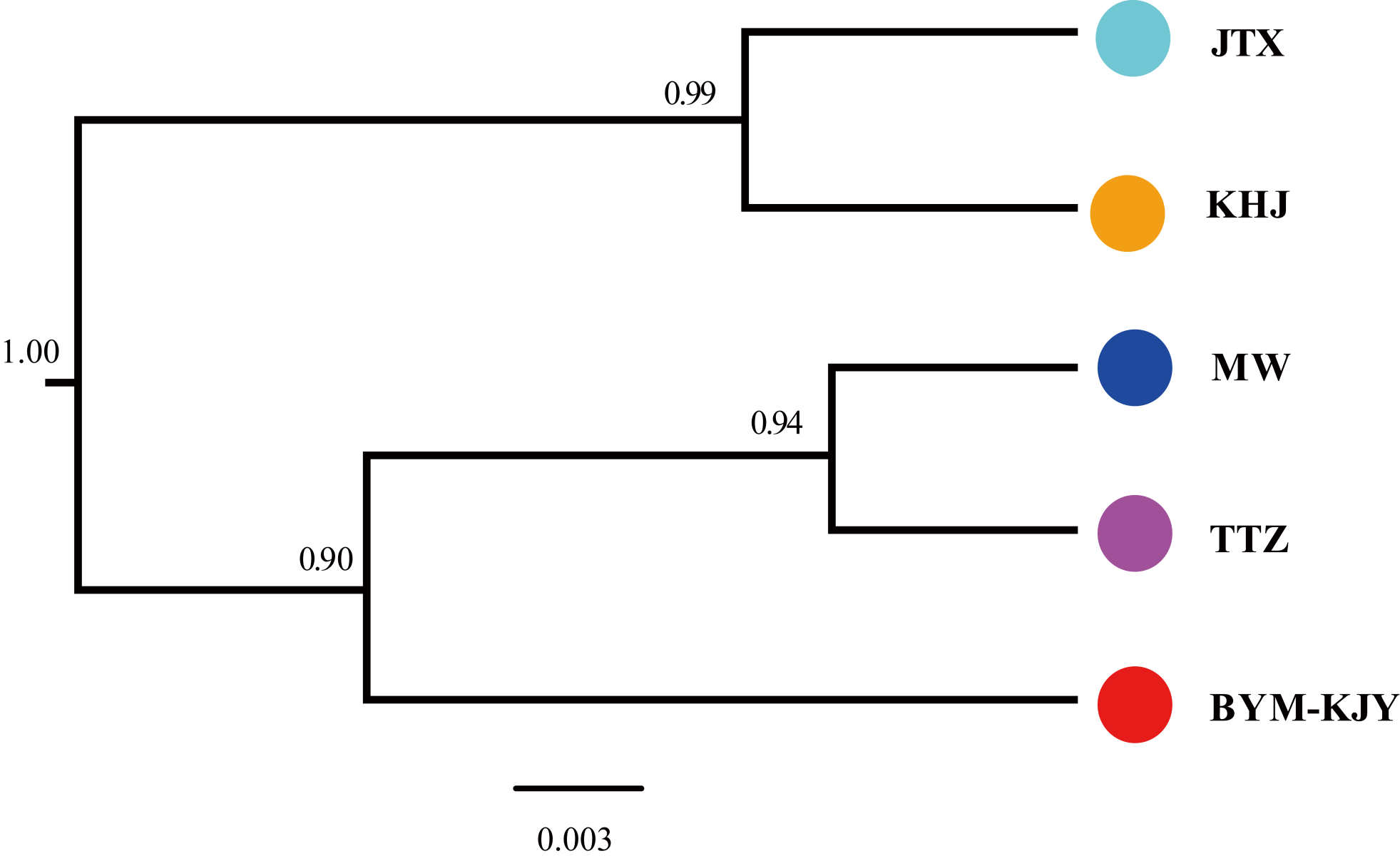


Table 1. The Species Delimitation results of *Pachyhynobius* in BF method.

Model	Species	MLE Path Sampling(PS)	MLE Stepping Stone(SS)	Rank	BF	
					PS	SS
M1	5	-34243.11	-34243.18	1	16.08	16.06
M2	4	-34251.15	-34251.21	2	-	-
M3	3	-34256.11	-34256.19	3	-	-
M4 (current taxonomy)	1	-34292.29	-34292.44	4	-	-

Note: “MLE”represents “Marginal likelihood estimate”; “BF ”represents “Bayes factor”.

Table 2. The species delimitation results of *Pachyhynobius* in BPP method.

Scheme	Priordistribution		Posterior probabilities
	θ	τ	
Scheme 1	G (1,10)	G (1,10)	P[5]=0.9971
Scheme 2	G (1,10)	G (1,100)	P[5]=0.9948
Scheme 3	G (1,10)	G (1,2000)	P[5]=0.9908
Scheme 4	G (1,100)	G (1,10)	P[5]=0.9984
Scheme 5	G (1,100)	G (1,100)	P[5]=0.9988
Scheme 6	G (1,100)	G (1,2000)	P[5]=0.9987
Scheme 7	G (1,2000)	G (1,10)	P[3]=1.0000
Scheme 8	G (1,2000)	G (1,100)	P[3]=1.0000
Scheme 9	G (1,2000)	G (1,2000)	P[3]=0.9999

Note: “P[5]” represents“((KHJ, JTX), (BYM-KJY, (TTZ, MW)))”; “P[3]” represents“(BYM-KJY-MW-TTZ, (KHJ, JTX))”.

Table 3. Number of lineages in *Pachyhynobius* inferred by multiple species delimitation methods.

Lineage	n	Mean Tamura–Nei distance	BF	GMYC single	GMYC multiple	bPTP	BPP	ABGD
JTX	8	0.001	1	1	2	1	1	1
KHJ	6	0.002	1	1	1	1	1	1
MW	6	0.003	1	1	1	1	1	1
TTZ	8	0.004	1	2	2	1	1	1
BYM-KJY	8	0.004	1	2	1	1	1	1
Total	36	0.0028	5	7 (5–14)	7 (5–7)	5.14(5–7)	5	5

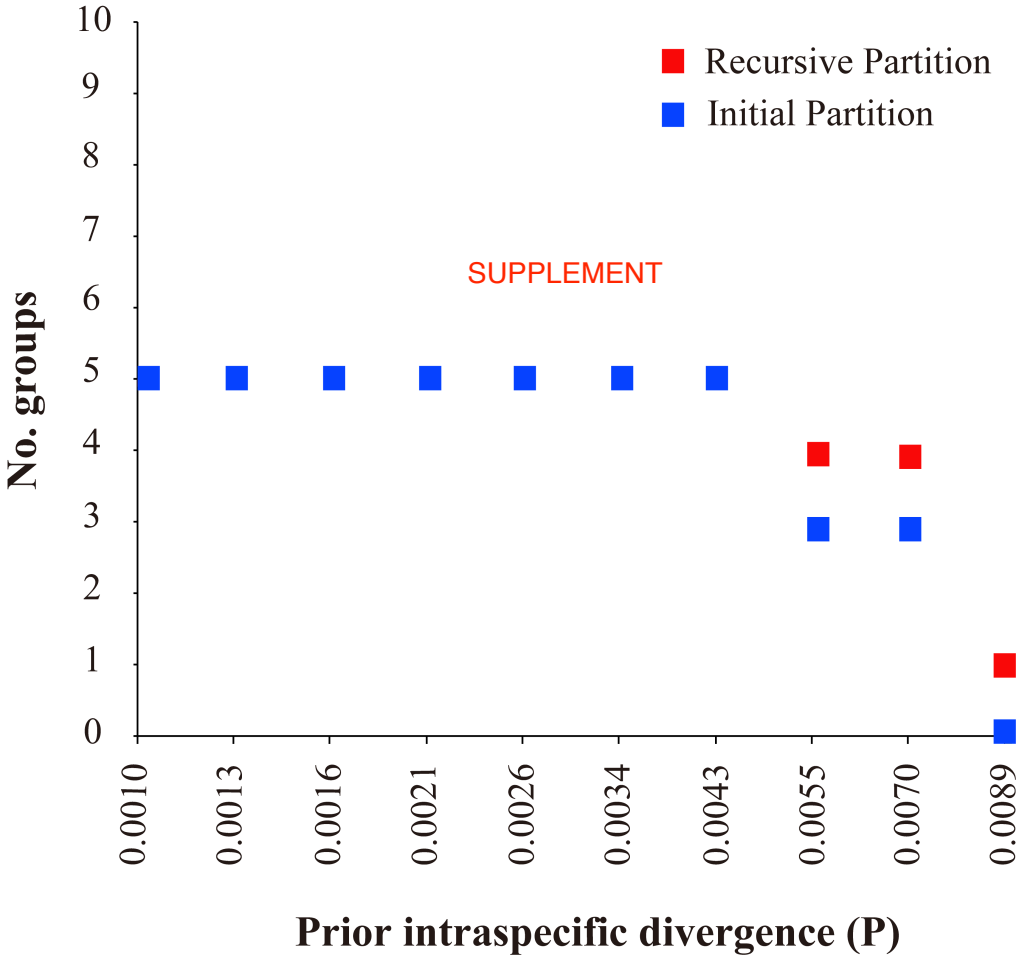
Note: “n” represents the number of individuals; All bPTP are from Bayesian MCMC analyses. Confidence intervals for totals are in parentheses.

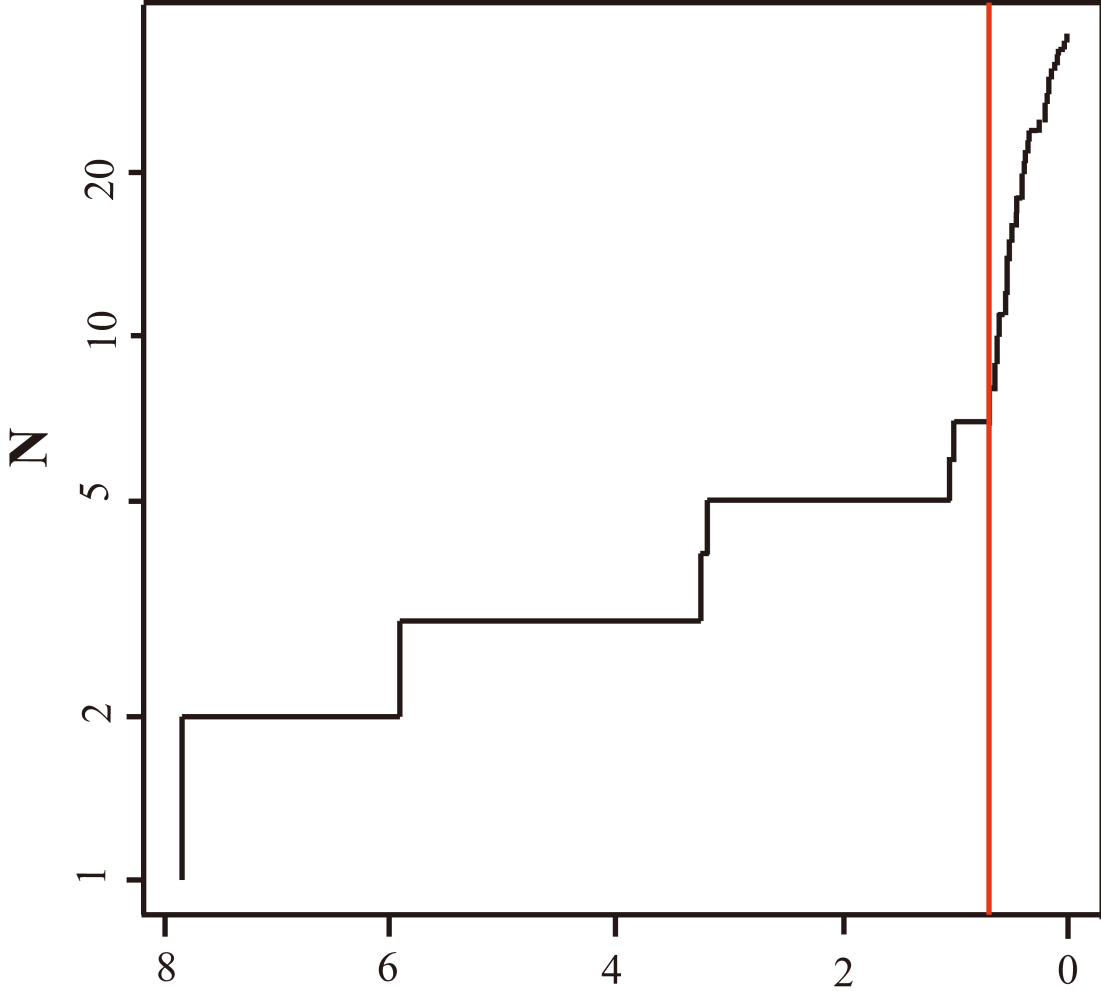
ABGD results are based on the initial partitioning scheme with a maximum intraspecific diversity value of 0.0055 (K80 distances).

Table 4. Pairwise F_{ST} among five candidate species (BYM-KJY, TTZ, MW, KHJ, JTX) of *Pachyhynobius*.

	BYM-KJY	TTZ	MW	KHJ	JTX
BYM-KJY					
TTZ	0.029*				
MW	0.031*	0.019*			
KHJ	0.039*	0.039*	0.041*		
JTX	0.037*	0.038*	0.039*	0.018*	

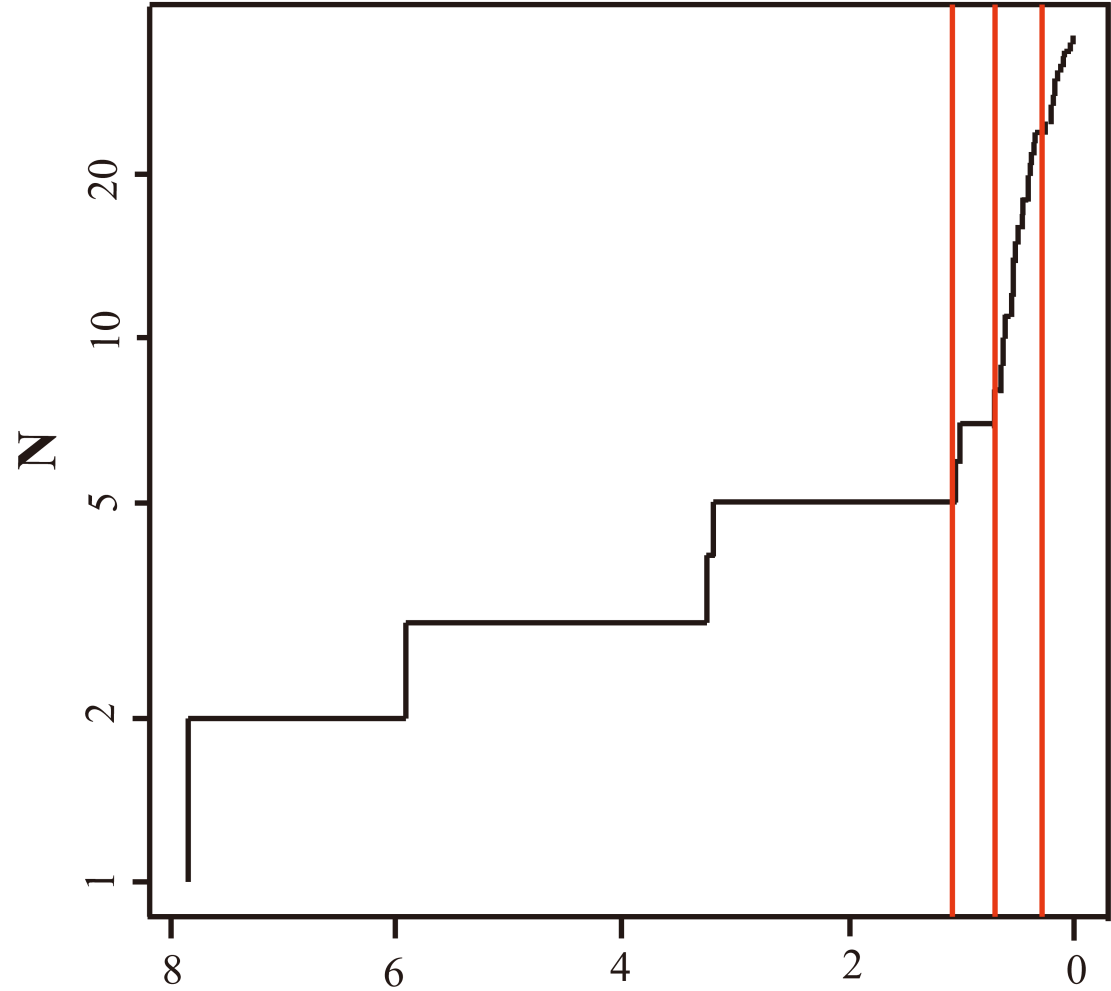
Note: Significant tests are indicated with an asterisk (* $P < 0.01$).





Time

A



Time

B

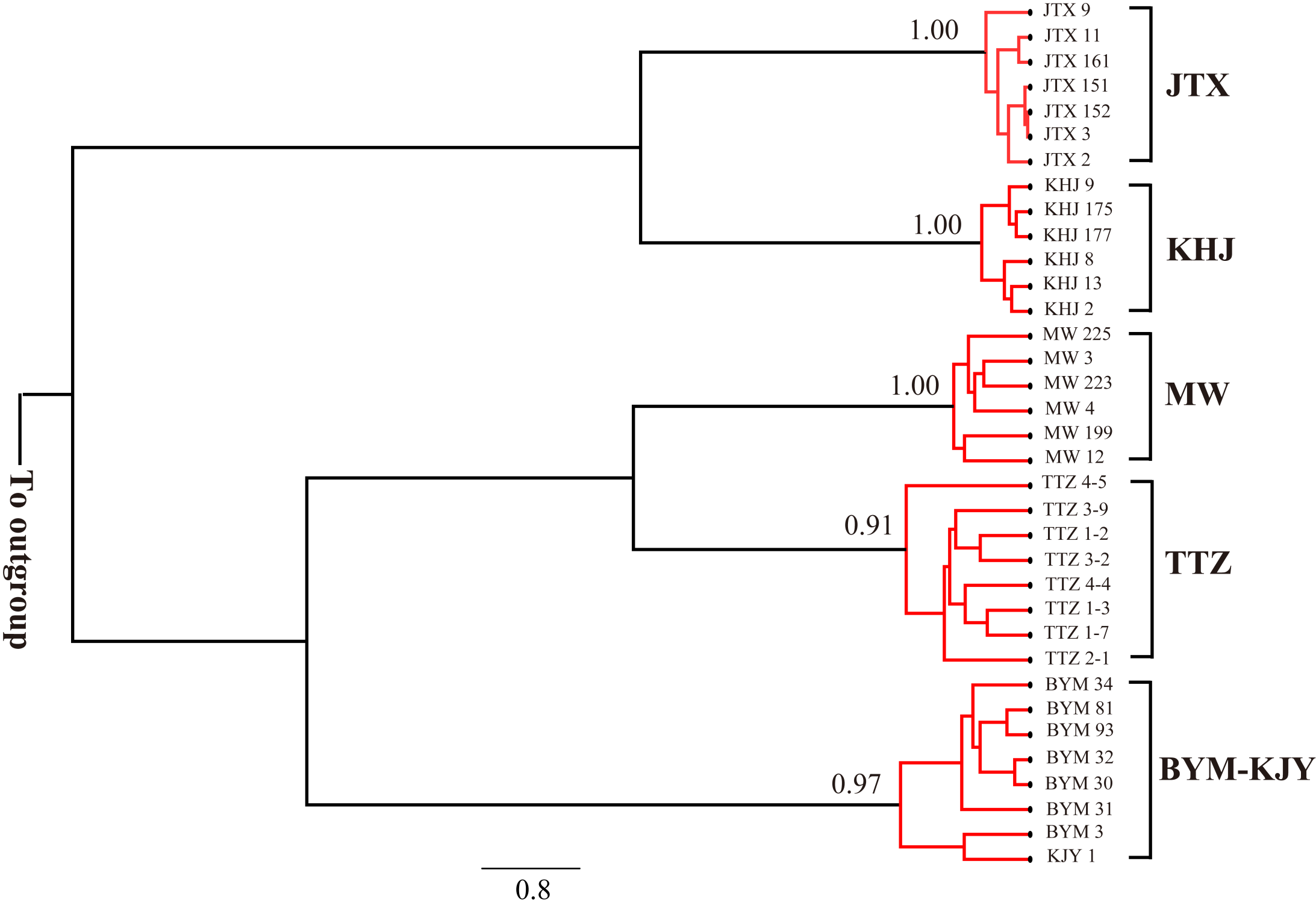


Table S1. Primers for amplified the complete mitochondrial genome of *Pachyhynobius*.

Pairs	Primer name	Sequence (5' to 3')	Gene	Annealing temp. (°C)
1	Psh-1F26	GTTTATGTAGCTTAAACAAAGCATGG	12S	53
	Psh-1R1333	TCGGAGTAGCTCGTTTAGTTTC	16S	53
2	Psh-2F1054	GCTTACACCAAGAAGATACTCGT	16S	53
	Psh-2R2363	GCTGTTATCCCTAGGGTAACTT	16S	53
3	Psh-3F2333	CGAGAAGACCCTATGGAGC	16S	53
	Psh-3R3363	AAGCTCTGATTCCCCTTCAGTT	ND1	53
4	Psh-4F3116	GGCTCAGGATGATCATCAAATC	ND1	53
	Psh-4R4326	CTATAGGTGCTAGTTTTTGTCAAGT	ND2	53
5	Psh-5F4065	AAACTTCATCACCCACGAGCAA	ND2	53
	Psh-5R5348	GTCATCGAGTGATTATCACAGGT	COX1	53
6	Psh-6F5067	CATCACCTGAATGCAACTCAGAT	COX1	53
	Psh-6R6348	CACAATATTGCGGCGTCTCATTT	COX1	53
7	Psh-7F6030	GACCCTGTACTTTACCAACATCT	COX1	53
	Psh-7R7478	ATACGAATTGGGGATTCTATTGGAA	COX2	53

8	Psh-8F7117	TCATGACCATGCATTAATAGCAGTTT	COX2	53
	Psh-8R8467	GCAATTAATTGAATTAATAAATGTCCGG	ATP6	53
9	Psh-9F8222	TCTAGGTTTATTACCATATACATTTACC	ATP6	53
	Psh-9R9359	CAACAAAATGTCAATATCATGCTGC	COX3	53
10	Psh-10F9106	GTAACCTGAGCTCATCATAGTATTAT	COX3	53
	Psh-10R10378	AATGGCGATGAAATAAAATCTACTCC	ND4	53
11	Psh-11F10137	AGGACTTGCATTAATAGTAGCTACT	ND4L	53
	Psh-11R11413	ATATACAATGTGTAGGAGGCTGTAAT	ND4	53
12	Psh-12F11181	CGCACTATTCTGCTTAGCAAATATAA	ND4	53
	Psh-12R12285	CTTGTATTGCTGCAGTATTTGCG	ND5	53
13	Psh-13F11928	GCATTTTAAATTAGCCTAACACCATTAA	ND5	53
	Psh-13R13168	CCTGAAACTATACTACCTCATGC	ND5	53
14	Psh-14F12941	GCACTCCATTTCTTGCTGGATTT	ND5	53
	Psh-14R14189	TTTTCGAATTGGGTGGGCCATTA	CYTB	53
15	Psh-15F13898	GCCAAAGAAGCAGAATACGCAAA	ND6	53
	Psh-15R15235	GATGCGGCTTGTCCAATTTCAAT	CYTB	53

16	Psh-16F14999	CTCATTACACCCCCACATATTCA	CYTB	53
	Psh-16R154	GGTCCTAGCCTTACTATTAATTGAAA	12S	53

Table S2 The complete mitochondrial genome of species in Hynobiidae with GeneBank accession nos. of corresponding sequences.

Taxonomy/Species name	Accession No.	Full Length(bp)
Order Caudata		
Family Hynobiidae		
<i>Batrachuperus londongensis</i>	NC008077	16,379
<i>B. pinchonii</i>	NC008083	16,390
<i>B. tibetanus</i>	NC008085	16,379
<i>B. yenyuanensis</i>	NC012430	16,394
<i>Hynobius amjiensis</i>	NC008076 (DQ333808)	16,401
<i>H. arisanensis</i>	NC009335 (EF462213)	16,401
<i>H. chinensis</i>	JQ710885	16,495
<i>H. chinensis</i> -CIB-XM2853	HM036353.1	16,404
<i>H. formosanus</i>	NC008084	16,394
<i>H. guabangshanensis</i>	NC013762	16,408
<i>H. kimurae</i>	JQ929920	16,448
<i>H. leechii</i>	NC008079 (DQ333811)	16,428
<i>H. maoershanensis</i>	NC023789	16,412
<i>H. nebulosus</i>	NC020650	16,447
<i>H. nigrescens</i>	NC026033	16,412
<i>H. quelpaertensis</i>	NC010224	16,407
<i>H. yangi</i>	NC013825	16,424
<i>H. yangi-l</i>	JN415127	16,403
<i>H. yiwuensis</i>	HM036354	16,494
<i>Liua shihi</i>	NC008078	16,376
<i>L. tsinpaensis</i>	NC008081	16,380
<i>L. tsinpaensis</i> –Tsinpa20141205	KP233806	16,378
<i>Onychodactylus fischeri</i>	NC008089	16,456
<i>O. zhangyapingi</i>	NC026853	16,537

<i>O. zhangyapingi</i> -1	KX021909	16,457
<i>O. zhaoermii</i>	KX021908	16,455
<i>Pachyhynobius shangchengensis</i>	NC008080	16,394
<i>P. shangchengensis</i> (JTX)	MK890394-MK890400	16,395-16,396
<i>P. shangchengensis</i> (KHJ)	MK890388-MK890393	16,393-16,394
<i>P. shangchengensis</i> (MW)	MK890382-MK890387	16,398-16,418
<i>P. shangchengensis</i> (TTZ)	MK890374-MK890381	16,397-16,400
<i>P. shangchengensis</i> (BYM)	MK890366-MK890370, MK890372, MK890373	16,396-16,399
<i>P. shangchengensis</i> (KJY)	MK890371	16,396
<i>Protohynobius puxiongensis</i>	FJ532058	16,398
<i>Pseudohynobius jinfo</i>	NC026698	16,393
<i>P. flavomaculatus</i>	NC020635	16,389
<i>P. puxiongensis</i>	NC020634	16,398
<i>P. shuichengensis</i>	NC021001	16,394
<i>P. tsinpaensis</i>	DQ333813	16,380
<i>Paradactylodon mustersi</i>	NC008090	16,383
<i>P. gorganensis</i>	NC008091	16,374
<i>Ranodon sibiricus</i>	NC004021	16,418
<i>Salamandrella keyserlingii</i>	DQ333814	16,338
<i>S. keyserlingii</i> -SK8321	JX508761	16,336
<i>S. keyserlingii</i> -SK8391	JX508762	16,340
<i>S. keyserlingii</i> -SK8440	JX508763	16,334
<i>S. keyserlingii</i> -SKN9	JX508764	16,338
<i>S. tridactyla</i>	NC021106	16,342
Order Caudata		
Family Cryptobranchidae		
<i>Andrias davidianus</i>	NC004926	16,503
<i>A. japonicus</i>	NC007446	16,298
